

## Separate-Local-Field NMR Spectroscopy on Half-Integer Quadrupolar Nuclei

Julia Grinshtein, Christopher V. Grant,<sup>†</sup> and Lucio Frydman\*

Department of Chemical Physics, Weizmann Institute of Sciences, 76100 Rehovot, Israel

Received June 24, 2002

Elements possessing half-integer quadrupolar nuclei are integral constituents in a variety of inorganic, organic, and biological structures.<sup>1</sup> The strong first-order quadrupolar anisotropy affecting these species generally restricts their solid-state NMR study to central-transition experiments.<sup>1,2</sup> The resulting resonances, however, will still be broadened by second-order quadrupole anisotropies. During the last years a number of 2D NMR alternatives have been proposed for the acquisition of high-resolution quadrupole resonances devoid of all anisotropy.<sup>3</sup> Upon employing these techniques to study the binding of metals to biomolecules, a variety of sites from polycrystalline samples have indeed been resolved.<sup>4</sup> Assigning these resonances to specific chemical motifs, however, is a challenging task on which efforts continue to be invested.<sup>5</sup> In fact similar challenges arose decades ago in the related field of high-resolution spin- $1/2$  solid-state NMR. Then, separate-local-field (SLF) MAS techniques exploiting the differential dipolar couplings which nuclei exhibit to their neighboring protons were found to be among the most practical routes to the unambiguous assignment of resonances.<sup>6</sup> Experiments monitoring heteronuclear couplings between  $^{13}\text{C}/^{15}\text{N}$  and  $^1\text{H}$ 's eventually became widely used resources in structural and dynamic characterizations of spin- $1/2$  spectra.<sup>7</sup> We report here on the potential arising when extending such SLF measurements to solid-state quadrupolar NMR.

Two main differences arise upon invoking SLF MAS techniques as aids in metal binding studies. The first is a consequence of the relatively long metal- $^1\text{H}$  distances in bioinorganic complexes, leading to SLF MAS sidebands that are typically too small to be observed. A second distinction arises from the inability of conventional MAS to remove the second-order anisotropies affecting quadrupolar line shapes. This implies that when applied as in spin- $1/2$  spectroscopy, quadrupolar 2D SLF MAS NMR will end up correlating second-order powder patterns along one axis, with dipolar sideband patterns along the other. These anisotropic-anisotropic 2D distributions will carry valuable information about the magnitudes and relative orientations between these two tensorial interactions, but lack the spectral resolution required for studying complex multisite systems.

A number of routes have been discussed on how to deal with the first of these problems; that is, the recoupling of quadrupolar and spin- $1/2$  nuclei subject to fast MAS.<sup>5,8</sup> A solution that we found particularly useful for implementing 2D SLF MAS NMR experiments is that which combines relatively fast sample spinning, with a  $2n\times$  magnification of the heteronuclear couplings based on  $\pi$ -pulses.<sup>9</sup> Figure 1 illustrates representative results observed upon applying these  $2n\times$  sequences to a  $^{23}\text{Na}$  SLF NMR analysis of  $\text{Na}_2\text{-dCMP}(5')\cdot 7\text{H}_2\text{O}$ . According to its X-ray structure this nucleotide possesses a unit cell with two inequivalent sodium sites in hexa-

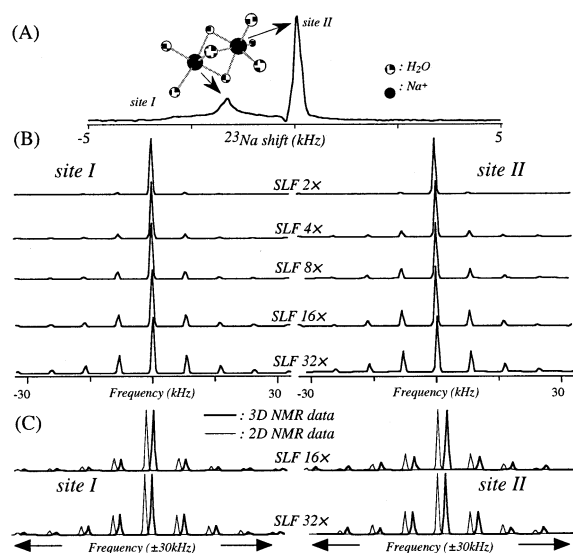


**Figure 1.** (A)  $^1\text{H}$ -decoupled  $^{23}\text{Na}$  NMR spectrum of  $\text{Na}_2\text{dCMP}(5')\cdot 7\text{H}_2\text{O}$ , showing the two inequivalent powder line shapes and their origin according to the diffraction structure. As for all remaining data this spectrum was collected on a laboratory-built 11.7 T NMR spectrometer at 8 kHz MAS, using a pulse sequence akin to that described in ref 9c. (B)  $^1\text{H}$ -dephasing progression exhibited by a series of  $2n\times$  MAS SLF acquisitions. (C) Comparison of  $16\times$  and  $32\times$  dipolar  $^1\text{H}$ - $^{23}\text{Na}$  SLF patterns resulting from 2D MAS- and 3D MQMAS-based pulse sequences (displaced for ease of visualization).

and penta-aquo coordination, forming a water-bridged dimer.<sup>10a</sup> This prediction is born out by the  $^{23}\text{Na}$  NMR data, which show a broader powder line shape that we assign to the pentacoordinated sodium environment and a sharper one from the more symmetric octahedral site (Figure 1A). These patterns can be resolved almost entirely by conventional MAS, giving us an opportunity for trying the SLF  $2n\times$  sequences in a 2D NMR fashion. Figure 1B illustrates  $^1\text{H}$ - $^{23}\text{Na}$  dipolar sideband line shapes obtained upon implementing such SLF MAS sequences on this deoxycytosine salt. A visual analysis evidences the ongoing magnification of the effective dipolar couplings with increasing  $n$  values, while confirming that the  $^{23}\text{Na}$  site coordinated in the more symmetric environment is subject to a stronger heteronuclear dipolar coupling.

A case like  $\text{Na}_2\text{dCMP}(5')\cdot 7\text{H}_2\text{O}$ , where heteronuclear dipolar couplings can be analyzed using conventional MAS methods, constitutes an exception rather than a rule. As mentioned earlier, MAS spectra will usually result in overlapping second-order powder patterns. To achieve site resolution in such cases, it becomes necessary to couple SLF MAS NMR with protocols capable of resolving inequivalent sites. Figure 2A illustrates an example of such merger with multiple-quantum magic-angle-spinning (MQMAS), resulting in a single 3D NMR sequence that resolves the dipolar/quadrupolar SLF MAS correlations for each inequivalent

\* To whom correspondence should be addressed. Fax: +972-8-9344123. E-mail: lucio.frydman@weizmann.ac.il.

<sup>†</sup> Current address: Department of Chemistry and Biochemistry, University of California-San Diego, 9500 Gillman Drive, La Jolla CA 92093.

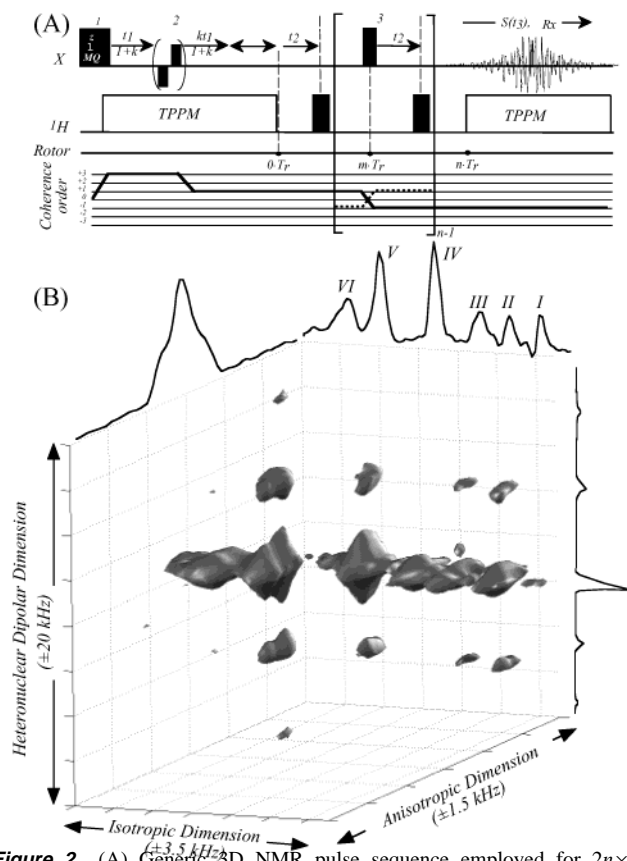


**Figure 2.** (A) Generic 3D NMR pulse sequence employed for  $2n \times$ -amplifications ( $n \geq 4$ ) of effective  $^1\text{H}-\text{X}$  local fields in combination with high-resolution MQMAS NMR. The sequence involves an initial split- $t_1$  delay encoding an isotropic evolution, a  $t_2$  labeling the  $^1\text{H}$  dipolar evolution, and a final  $t_3$  acquisition under conventional MAS. In the experimental  $\text{X} = ^{23}\text{Na}$  implementation  $\phi_1$  was incremented in  $30^\circ$  steps,  $\phi_2$  was kept constant,  $\phi_3$  was incremented in  $180^\circ$ , and  $\phi_{\text{Rx}}$  was cycled to retrieve the illustrated coherence transfer pathway. (B) Isosurface representation of a  $16 \times$  SLF MQMAS 3D  $^{23}\text{Na}$  NMR spectrum recorded for  $\text{Na}_2\text{UMP}(3') \cdot 4\text{H}_2\text{O}$ , showing the projections resulting along the three orthogonal spectral axes. Data were recorded using 32, 8, and 64 total  $t_1$ ,  $t_2$ , and  $t_3$  points; 250, 6.25, and 62.5  $\mu\text{s}$  dwell times along  $t_1$ ,  $t_2$ , and  $t_3$ ; an echo delay  $\Delta = 2$  ms ( $32 \cdot T_r$ ) centering the time-domain data along  $t_3$ ; a  $9.3 \mu\text{s}$  3Q excitation pulse, and an optimized  $3\text{Q} \rightarrow 1\text{Q}$  FAM conversion.<sup>11</sup> Because of the amplitude modulation occurring along  $t_2$  and the echo arising along  $t_3$ , purely absorptive data sets ( $128^3$  points) were obtained on Fourier processing a single experimental 3D data set.

site in the sample. Such sequence yields  $^1\text{H}-^{23}\text{Na}$  dipolar sideband patterns that are indistinguishable from their conventional 2D NMR counterparts (Figure 1C). Figure 2B summarizes the NMR results obtained when applying such sequence on the multisite  $\text{Na}_2\text{UMP}(3') \cdot 4\text{H}_2\text{O}$  nucleotide. According to its X-ray study this nucleotide should present two chemically inequivalent sodium atoms,<sup>10b</sup> but when it was recrystallized as described in the literature, six resonances were consistently observed in its high resolution  $^{23}\text{Na}$  MQMAS NMR spectrum. Figure 3 illustrates the  $^1\text{H}-^{23}\text{Na}$  dipolar patterns that resulted from 3D MQMAS SLF NMR measurements obtained as a function of dipolar amplification factor, for all the six sites resolved in this uridine sample. Variations in heteronuclear coupling strengths are clearly picked up by this new 3D NMR experiment for the various sites, and characteristic changes in these dipolar MAS spectra were also observed upon increasing the coupling's magnification. A refined multispin numerical analysis indicates that this dipolar sideband pattern progression is sensitive to the actual coordination number and to the geometry surrounding the metal ion. This can help us define metal-binding environments

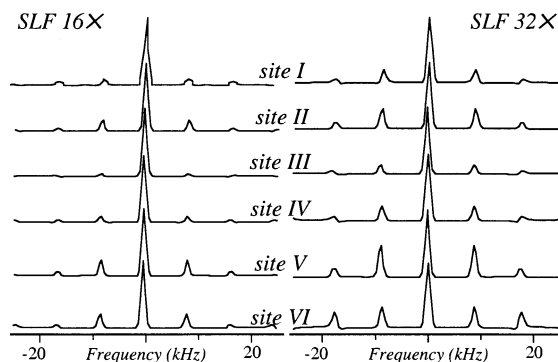


**Figure 3.**  $^1\text{H}-^{23}\text{Na}$  dipolar MAS sideband patterns resolved for the six sites of polycrystalline  $\text{Na}_2\text{UMP}(3') \cdot 4\text{H}_2\text{O}$ , labeled as in Figure 2. These 3D NMR experiments were recorded using the sequence illustrated in that Figure, with  $16 \times$  and  $32 \times$  dipolar amplification factors.

in samples that, like this one, have eluded crystallographic analyses, as will be detailed in a more comprehensive publication.

**Acknowledgment.** We thank Dr. V. Frydman for the preparation of the nucleotide samples. This work was supported by a Philip M. Klutznick Fund for Research, by the Israeli Science Foundation (Grant No. 296/01), and by NIH Postdoctoral Fellowship GM 20417 (CVG).

## References

- (1) (a) Anderson, M. W.; Duer, M. J., Eds. *New NMR Techniques for Quadrupolar Nuclei*. *Solid State NMR* **1999**, *15*. (b) Smith, M. E.; vanEck, E. R. H. *Prog. Nucl. Magn. Reson. Spectrosc.* **1999**, *34*, 159. (c) *Solid State NMR of Inorganic Materials*; Fitzgerald, J., Ed.; ACS Symposium Series 717; American Chemical Society: Washington, DC, 1999.
- (2) (a) Cohen, M. H.; Reif, F. *Solid State Phys.* **1957**, *5*, 321. (b) Abragam, A. *Principles of Nuclear Magnetism*; Oxford University Press: Oxford, 1961.
- (3) (a) Mueller, K. T.; Sun, B. Q.; Chingas, G. C.; Zwanziger, J. W.; Terao, T.; Pines, A. *J. Magn. Reson.* **1990**, *86*, 470. (b) Frydman, L.; Harwood, J. S. *J. Am. Chem. Soc.* **1995**, *117*, 5367. (c) Medek, A.; Harwood, J. S.; Frydman, L. *J. Am. Chem. Soc.* **1995**, *117*, 12779. (d) Gan, Z. H. *J. Am. Chem. Soc.* **2000**, *122*, 3242.
- (4) For instance: (a) Grant, C. V.; Frydman, V.; Frydman, L. *J. Am. Chem. Soc.* **2000**, *122*, 11743. (b) Ashenurst, J.; Wang, S.; Wu, G. *J. Am. Chem. Soc.* **2000**, *122*, 3528. (c) Rovnyak, D.; Baldus, M.; Wu, G.; Hud, N. V.; Feigon, J.; Griffin, R. G. *J. Am. Chem. Soc.* **2000**, *122*, 11423.
- (5) For instance: (a) Wang, S. H.; DePaul, S. M.; Bull, L. M. *J. Magn. Reson.* **1997**, *125*, 364. (b) Fernandez, C.; Lang, D. P.; Amoureux, J.-P.; Pruski, M. *J. Am. Chem. Soc.* **1998**, *120*, 2672. (c) Duer, M. J.; Painter, A. J. *J. Chem. Phys. Lett.* **1999**, *313*, 763. (d) Dowell, N. G.; Ashbrook, S. E.; McManus, J.; Wimperis, S. *J. Am. Chem. Soc.* **2001**, *123*, 8135. (e) Lupulescu, A.; Brown, S. P.; Spiess, H. W. *J. Magn. Reson.* **2002**, *154*, 101. (f) Edén, M.; Grinshtein, J.; Frydman, L. *J. Am. Chem. Soc.* **2002**, *124*, 9708.
- (6) (a) Opella, S. J.; Frey, M. H. *J. Am. Chem. Soc.* **1979**, *101*, 5854. (b) Munowitz, M. G.; Griffin, R. G.; Bodenhausen, G.; Wang, T. H. *J. Am. Chem. Soc.* **1981**, *103*, 2529. (c) Munowitz, M. G.; Griffin, R. G. *J. Chem. Phys.* **1982**, *76*, 2848. (d) Schaefer, J.; McKay, R. A.; Stejskal, E. O.; Dixon, W. T. *J. Magn. Reson.* **1983**, *52*, 123. (e) Webb, G. G.; Zilm, K. W. *J. Am. Chem. Soc.* **1989**, *111*, 2455.
- (7) For instance: (a) Fyfe, C. A. *Solid State NMR for Chemists*; CFC Press: Ontario, 1983. (b) McBrierty, V. J.; Packer, K. J. *Nuclear Magnetic Resonance in Solid Polymers*; Cambridge University Press: Cambridge, 1993. (c) Schmidt-Rohr, K.; Spiess, H. W. *Multidimensional Solid-State NMR and Polymers*; Academic Press: London, 1994. (d) Stejskal, E. O.; Memory, J. D. *High-Resolution NMR in the Solid State: Fundamentals of CPMAS*; Oxford University Press: New York, 1994.
- (8) For instance: (a) Gullion, T. *Chem. Phys. Lett.* **1995**, *246*, 325. (b) Grey, C. P.; Vega, A. J. *J. Am. Chem. Soc.* **1995**, *117*, 8232. (c) Chopin, L.; Vega, S.; Gullion, T. *J. Am. Chem. Soc.* **1998**, *120*, 4406.
- (9) (a) Hong, M.; Gross, J. D.; Rienstra, C. M.; Griffin, R. G.; Kumashiro, K. K.; Schmidt-Rohr, K. *J. Magn. Reson.* **1997**, *129*, 85. (b) McElheny, D.; deVita, E.; Frydman, L. *J. Magn. Reson.* **2000**, *143*, 321. (c) deVita, E.; Frydman, L. *J. Magn. Reson.* **2001**, *148*, 327.
- (10) (a) Pandit, J.; Seshadri, T. P.; Viswamitra, M. A. *Acta Crystallogr.* **1983**, *C39*, 342. (b) Viswamitra, M. A.; Reddy, B. S.; James, M. N. G.; Williams, G. J. B. *Acta Crystallogr.* **1972**, *B28*, 1108.
- (11) (a) Madhu, P. K.; Goldbourt, A.; Frydman, L.; Vega, S. *Chem. Phys. Lett.* **1999**, *307*, 41. (b) Madhu, P. K.; Goldbourt, A.; Frydman, L.; Vega, S. *J. Chem. Phys.* **2000**, *112*, 2377.

JA020882X